

Article

# Influence of Stratigraphic Conditions on the Deformation Characteristics of Oil/Gas Wells Piercing Longwall Pillars and Mining Optimization

Shun Liang <sup>1,2,3</sup>, Derek Elsworth <sup>2</sup>, Xuehai Fu <sup>3,\*</sup>, Xuehua Li <sup>1</sup> and Qiangling Yao <sup>1</sup>

<sup>1</sup> School of Mines, Key Laboratory of Deep Coal Resource Mining, Ministry of Education, China University of Mining and Technology, Xuzhou 221116, China; liangshun@cumt.edu.cn (S.L.); lsxh2001@126.com (X.L.); yaoqiangling@cumt.edu.cn (Q.Y.)

<sup>2</sup> EMS Energy Institute, G3 Center and Energy and Mineral Engineering, Pennsylvania State University, University Park, State College, PA 16802, USA; elsworth@psu.edu

<sup>3</sup> Key Laboratory of Coalbed Methane Resource and Reservoir Formation Process, Ministry of Education, China University of Mining and Technology, Xuzhou 221008, China

\* Correspondence: fuxuehai@163.com; Tel.: +86-516-8359-0165

Academic Editor: Mofazzal Hossain

Received: 18 April 2017; Accepted: 31 May 2017; Published: 3 June 2017

**Abstract:** Hydrocarbon wells drilled vertically through longwall coal pillars are vulnerable to severe deformation and potential failure as a result of underground coal mining. The lithology of the host rocks play a critical role in well stability. In this study, a two dimensional finite element method is employed to investigate the horizontal shear offset, vertical delamination, and compression at the weak interface between neighboring soft and stiff layers after the sequential extraction of longwall panels flanking the protective coal pillar. The influence of stratigraphic conditions, including the single rock layer thickness (SRLT), seam mining height (SMH), and seam dip angle (SDA), on deformation of hydrocarbon wells is explored. An optimization of mining sequence along strike and for panel advance direction along dip is also performed. Finally, some recommendations regarding coal mining and peripheral support measures are suggested.

**Keywords:** hydrocarbon wells; rock layer thickness; seam mining height; seam dip angle; well stability; longwall mining

## 1. Introduction

The success of horizontal drilling and hydraulic fracturing in tapping deep shale gas reservoirs has resulted in the need for wells to successfully transit coal seams that may ultimately be mined. To successfully maintain the yield of the wells that act as the conduits for the transmission of hydrocarbon resources from the underground reservoir to the surface, it is critical to ensuring the stability and security of these hydrocarbon wells during their service life. However, in some sedimentary basins where coal, gas and oil coexist, such as the Ordos basin, China, and the Appalachian Basin, in the United States, ensuring the stability of wells traversing coal seams is becoming a daunting challenge, adversely impeding the simultaneous recovery of coal and hydrocarbon resources [1–8]. The extensive and intense strata movement and deformation induced by longwall coal mining may result in large deformations and potential failure of the hydrocarbon wells. If the wells are improperly designed, longwall-mining-induced wellbore deformation or failure could have a significant adverse impact on well yield, or even in worse cases, resulting in the entrance of oil/gas into the aquifer, polluting ground water [9,10]. Moreover, the fugitive hydrocarbon gas could enter into the adjacent coal faces, triggering catastrophes like gas explosion and mine conflagration [11,12]. All of these severely endanger mine safety and the local ecological, geological, and environmental systems. For example, on 29 April 2006,

a gas explosion accident occurred at the Wayaobao colliery located in the Zichang oilfield in China, as a result of the uncovering of an unknown abandoned gas well using blast mining. This tragic incident caused 32 deaths and seven injuries, with an immediate economic loss of 1.5 million US dollars. Therefore, it is of critical importance to guarantee the integrity of hydrocarbon wells piercing longwall mining areas to ensure the safe simultaneous extraction of coal and hydrocarbon resources.

A wealth of observations indicates that the geological conditions that the oil/gas wells penetrate are of critical significance to their integrity. The effect of longwall mining on an oil/gas well is determined by seam burial depth, abutment pressure, pillar size and location of the well with respect to panel edges [6,13]. Liang [14] classified the factors controlling the stability of hydrocarbon wells vertically drilled through longwall mining areas into three categories: (1) geological factors, including seam burial depth, overburden lithology, single rock layer thickness (SRLT), ground stress intensity and orientation, seam dip angle (SDA), special geological structures (e.g., fault fold structure), surface topography, and ground water; (2) coal seam mining factors, including seam mining height (SMH), mining method, roof control method, panel layout (along strike or dip), panel advance rate and direction (updip mining or downdip mining), mining sequence, panel dimension, and protective pillar dimension; (3) wellbore construction factors, including well location, drilling method, drilling fluid density, directional drilling, casing material and performance. Among them, stratigraphic conditions play a critical role in determining the scale and scope of the mining influence. Thicker and stiffer rock layers within the overlying strata are less likely to fracture [15–18]. As a result, hydrocarbon wells drilled through these rock layers are more prone to remain stable. Increasing SMH provides more space for the movement and readjustment of the overburden rocks after panel removal, resulting in greater strata movement and deformation. As for SDA, its influence is mainly manifest at weak interfaces between soft and stiff layers. In other words, in the case of an inclined coal seam, shear slip is more likely to occur at the weak interfaces under the action of self-weight of the overburden rocks, thus posing a hazard to the integrity of hydrocarbon wells.

Abundant studies report the analysis of well and casing stability under the primitive stress field (free from underground excavations) including wellbore stability during drilling. Many failure mechanisms [19–25] and detailed drilling optimizations [26–29] are described. However, few studies exist with regard to the failure of hydrocarbon wells subject to underground longwall coal mining. Prior studies have examined the stability of wells piercing longwall mining areas in the Appalachian Basin in the US. The previous studies include an examination of: (1) topographic influence on stability for gas wells penetrating longwall mining areas [3]; and (2) dynamic impacts on gas wells during the advance of the twin panels flanking the central protective coal pillar [4]. Actually, longwall-induced deformations are site-specific and more study is needed to completely characterize the induced deformations under different geological and mining conditions [7]. In this study, we present a 2D model to examine the influence of SRLT, SMH and SDA on the critical deformations (horizontal shear offset, vertical delamination/bed separation and compression) controlling the stability of hydrocarbon wells vertically traversing through longwall mining areas. A supplementary 3D model optimizes the mining sequence of longwall mining along strike and the direction of longwall mining relative to dip, thus minimizing the damage to the wells. Finally, we make several suggestions on panel extraction methods favoring the stability of hydrocarbon wells in longwall mining areas, along with suitable safeguard measures.

## 2. Background and Methodology

Hydrocarbon wells transiting coal seams fail mainly as a result of intense strata movement and deformation induced by coal seam longwall mining. Well deformation is manifest in different forms, including: (1) tensile and compressional failure within the strata along the horizontal and vertical direction, and distortion deformation along the wellbore axis; (2) distortion deformation at interfaces between beds resulting from the combined action of shear, tensile (delamination) and compressional deformation. Among these deformations, hydrocarbon wells are most susceptible to failure triggered

by excessive shear and distortion at interfaces between soft and stiff layers [3,7,30–34]. This paper employs a 2D model to perform a parametric study of the influence of stratigraphic conditions on the deformation characteristics of hydrocarbon wells in longwall mining areas, with an emphasis on deformations between adjacent beds with contrasting lithology.

### 2.1. Strata and Well Deformation

Strata deformation occurs as a result of the changes of stress distribution within the rock mass. The stress change at the interfaces between adjacent beds with dissimilar rock properties and induced by longwall mining is one reason for the incompatible deformation of twin layers flanking the interface. A 2D FLAC<sup>®</sup> model is used to represent the large displacement of the medium. An interface element is used in the model to faithfully characterize the mining-induced response occurring at this weak interface between the soft and stiff layer. We idealize the subsurface as a deformable medium comprised of alternating soft and stiff beds with a separating weak interface characterized by an interface element. This element allows horizontal slip, vertical delamination (bed separation) and compression at the weak interfaces. Figure 1 illustrates the typical deformation modes of a hydrocarbon well in and between layers of alternating soft shale and stiff sandstone as the well is distorted by longwall-induced movement.

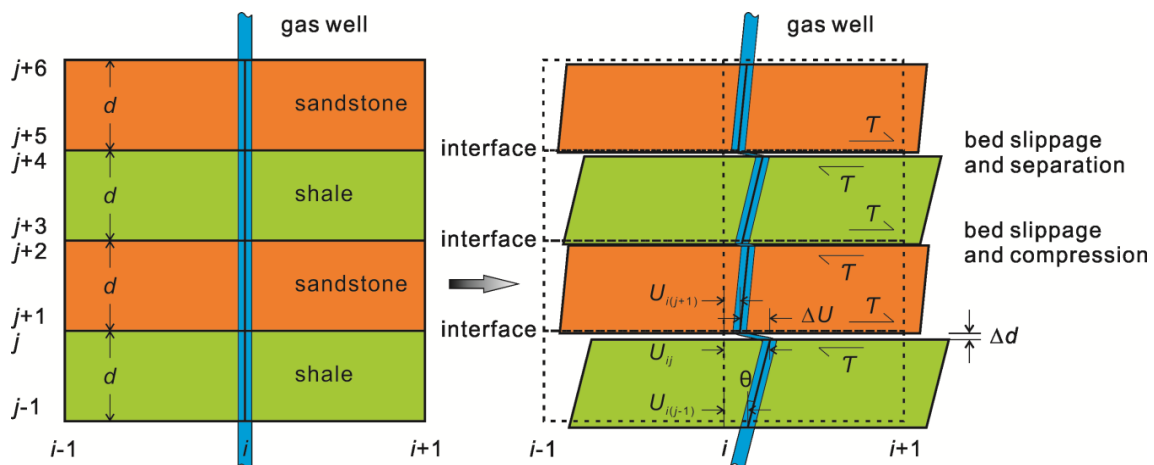


**Figure 1.** Typical deformation of an oil/gas well in and between layers of alternating soft rock and stiff rock as the well is distorted by longwall-induced movement (with slip interfaces between alternating layers) [3].

We represent this interface between layers of alternating mechanical properties by an interface element (Figure 1), where the elastic distortion,  $\epsilon_e$ , irrecoverable shear slip distortion (intrastratal distortion),  $\epsilon_i$ , and total distortion,  $\epsilon_t = \epsilon_e + \epsilon_i$  are defined as:

$$\begin{aligned} \epsilon_e &= \frac{U_x}{d} = \frac{U_{ij} - U_{i(j-1)}}{d} \\ \epsilon_i &= \frac{\Delta U}{\Delta d} = \frac{U_{i(j+1)} - U_{ij}}{\Delta d} \\ \epsilon_t &= \frac{T_x}{d} = \frac{U_{i(j+1)} - U_{i(j-1)}}{d} \end{aligned} \tag{1}$$

where,  $U_x$  is the intra-strata elastic shear offset;  $\Delta U$  is interlaminar relative shear offset;  $T_x = U_x + \Delta U$  is total offset and is normalized over the bed thicknesses;  $d$  and  $\Delta d$  separately refer to SRLT and the vertical separation distance between layers ( $\Delta d > 0$  indicating delamination (bed separation), while  $\Delta d < 0$  indicating compression);  $U_{ij}$  denotes the lateral shear offset of node  $(i, j)$ , with a similar meaning for  $U_{i(j-1)}$  and  $U_{i(j+1)}$ .

## 2.2. Geological Setting and Mining Parameters

The geological setting of coal mines in southwest Pennsylvania (e.g., Cumberland, Emerald, and Clyde), is assumed in this study as a comprehensive description of coal measure rocks, worldwide. In recent years, the three-entry system (two rows of protective pillars) has gained dominance in the longwall panel designs in this region. Mining activities at the above coal mines are primarily performed in the Pittsburgh coal seam, which is 1.5–2.5 m in thickness. At a depth of 280 m, the seam is near horizontal. Longwall mining and room-and-pillar mining are widely employed by coal mines in this area, with longwall mining producing over 80% of the coal. A longwall panel is typically 350–450 m wide and over 2000 m long, with the longest panels reaching 4000 m. In general, a 50 m wide chain pillar, termed a protective pillar for hydrocarbon wells in this study, is reserved between the two adjacent longwall panels. This chain pillar is separated by a 5 m wide gate road into two parts, namely a 15 m wide yield pillar and 30 m wide barrier pillar, as shown in Figure 2.

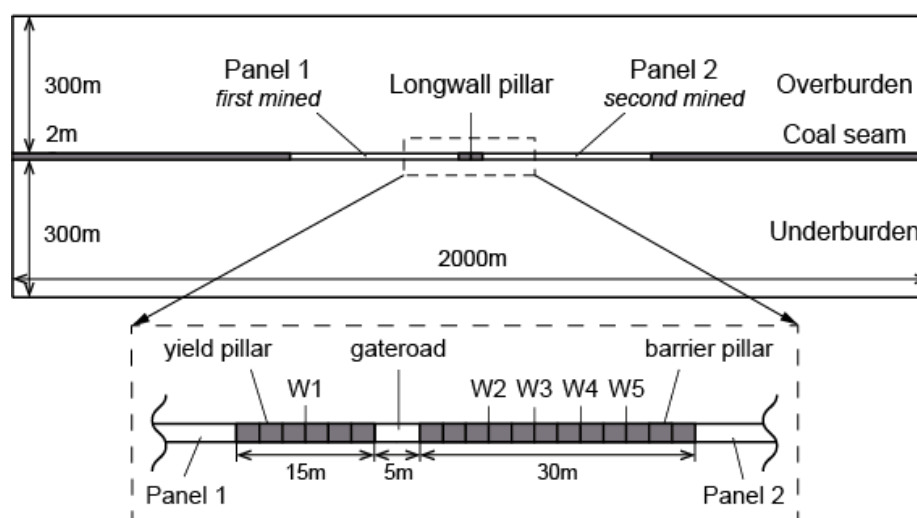


**Figure 2.** Schematic diagram of the base model (Pillar geometry between the twin extracted panels is shown in the excerpted frame. Panel 1 is removed first and then panel 2 is removed afterwards.).

## 2.3. Model

Strata overlying the Pittsburgh coal seam mainly comprise layered strong sandstone and limestone and relatively weak shales [35,36]. The stratigraphic column, extrapolated from three typical geological boreholes indicates that single rock layers within the strata are mainly 3–23 m thick, among which hard/stiff layers (sandstone and limestone) have an accumulative thickness that accounts for 33–45% in total strata thickness. Therefore, the following simplifications are made in the numerical model: (1) the strata are comprised of alternating soft and stiff layers; (2) the soft layer and stiff layers are in the proportion 50% and 50% in height, separately.

To fully examine of influence of SRLT, SMH and SDA on deformation characteristics of hydrocarbon wells penetrating longwall mining areas, a 2000 m wide two dimensional geological model is established as the base model (later-mentioned as scenario I-2), where the 2 m thick coal seam and 300 m thick overlying and underlying strata are positioned horizontally. The overlying strata are comprised of alternating strong/stiff sandstone and weak/soft shale with the same thickness of 10 m. The longwall panel is 370 m wide, advancing along the axis perpendicular to the plane of the figure. The left panel is the first to be extracted, followed by the right panel. The upper boundary is stress-free, the basal boundary is fixed in the vertical direction, and the lateral boundaries are fixed in the horizontal direction. Governed by a Mohr-Coulomb criterion, the model runs to an initial equilibrium loaded by gravity.

Compared to well stability under primitive stress conditions (free from underground excavations), longwall-induced strata movement poses a more severe influence on the stability of hydrocarbon wells traversing coal seams. The vertical well trajectory is not included in the global model, as its resistance is small in comparison to the unrestrained deformations of the strata (e.g., [13]). Instead, five measuring lines that pierce the pillar define the five candidate well trajectories (W1–W5, Figure 2). In the figure, each element comprising the coal pillar is 2.5 m wide. Well horizontal shear offset and vertical delamination and compression as well as the combined distortion at interfaces between beds are characterized by the horizontal and vertical relative displacement of the two nodes on the measuring line at the weak interface between adjacent beds.

To specifically explore the influence of SRLT, SMH and SDA on deformation characteristics of hydrocarbon wells, we modify the SRLT, SMH and SDA in successive simulations. This is based on the base model (scenario I-2). As a result, three study groups are designed, with each study group containing three or four sub-scenarios. It should be noted that the burial depth of the coal seam (for protective pillar) in Group III is taken as 900 m so as to allow for the adjustment of the seam dip angle (SDA). The stratigraphic conditions for each scenario are detailed in Table 1. The mechanical parameters of rocks and interfaces used in the model [3,5], which are summarized in Table 2. The influence of SRLT, SMH and SDA on the deformation and stability of hydrocarbon wells is examined through comparison of mining-induced well deformations in various scenarios.

**Table 1.** Numerical modeling scenarios to define the influence of various stratigraphic factors on well deformations.

Study Group	Scenario	SRLT (m)	SMH (m)	SDA (°)	Seam Burial Depth (m)
Group I	I-1	5	2	0	300
	I-2	10			300
	I-3	20			300
Group II	II-1	10	1	0	300
	II-2 (I-2)		2		300
	II-3		3		300
	II-4		4		300
Group III	III-1	10	2	0	900
	III-2			8	900
	III-3			16.7	900
	III-4			31	900

**Table 2.** Mechanical parameters of rocks and interfaces used in the model (scheme I-2 as an example).

Lithology	Thickness (m)	Cumulative Thickness (m)	Bulk K (GPa)	Shear G (GPa)	Density $\rho$ (Kg/m <sup>3</sup> )	Cohesion <i>c</i> (MPa)	Friction Angle $\Phi$ (°)	Tension $\sigma_t$ (MPa)
-	280	300	Alternating layers of soft shale and stiff sandstone in overburden					
Sandstone/limestone	10	302	13.3	8.0	2650	88	30	1.0
Shale/mudstone	10		3.3	2.0	2300	21	30	0.4
Coal seam	2.0		2.3	1.4	1500	1.5	30	0.01
Shale/mudstone	10		3.3	2.0	2300	21	30	0.4
Sandstone/limestone	10		13.3	8.0	2650	88	30	1.0
-	280	602	Alternating layers of soft shale and stiff sandstone in underburden					
<b>Mechanic Properties of Interfaces between Adjacent Beds</b>								
Shear Stiffness $K_s$ (MPa)			Normal Stiffness $K_n$ (MPa)			Friction Angle $\phi$ (°)		
17			17			20		

### 3. Analysis of Model Results

Field observations and previous studies define that horizontal shear offset and vertical delamination or compression at weak interfaces between adjacent soft and stiff layers in the overburden,

as well as the intra-stratal distortion resulting from combined deformation are the most damaging to traversing wells/boreholes [3,5,31,34]. It is concluded that hydrocarbon wells are most susceptible to failure at coal seam and bedding interfaces proximal to the roof and floor strata, where the magnitude of shear, distortion and compression is the largest. Therefore, in this study we only record the peak magnitude of horizontal shear offset and vertical delamination and compression of the wells in each scenario. These are then used to examine the influence of SRLT, SMH and SDA.

### 3.1. Influence of Single Rock Layer Thickness (SRLT)

In the first study group (I-1–I-3), SRLT is selected as 5, 10 and 20 m, respectively. Seam burial depth and seam thickness are fixed at 300 and 2 m, respectively for a horizontal seam. Lateral shear offset, delamination and compression of the five candidate well trajectories after sequential extraction of the panels flanking the central pillar are separately plotted in Figures 3 and 4.

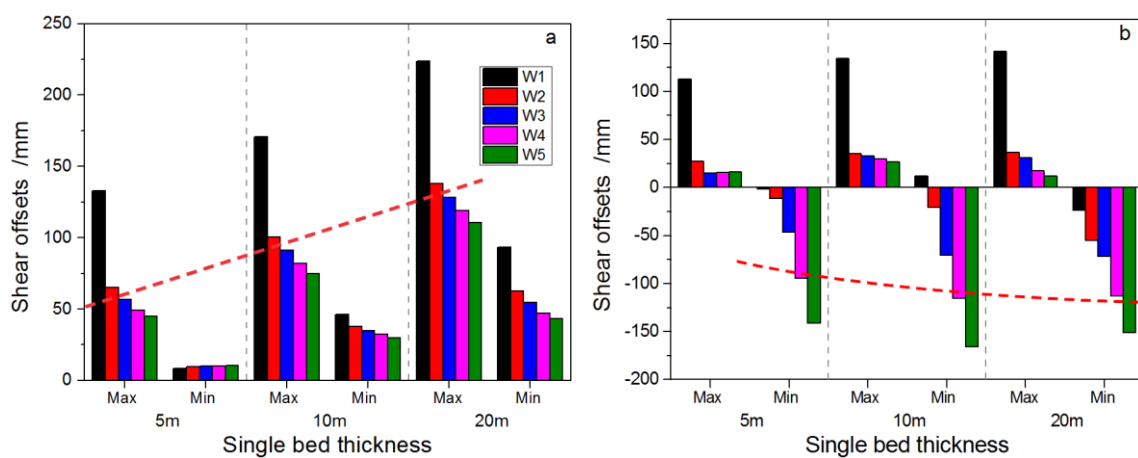


**Figure 3.** Extreme value statistics of horizontal shear offsets of hydrocarbon wells after the (a) first panel is removed and then (b) twin panels are removed sequentially in the cases of various SRLTs.

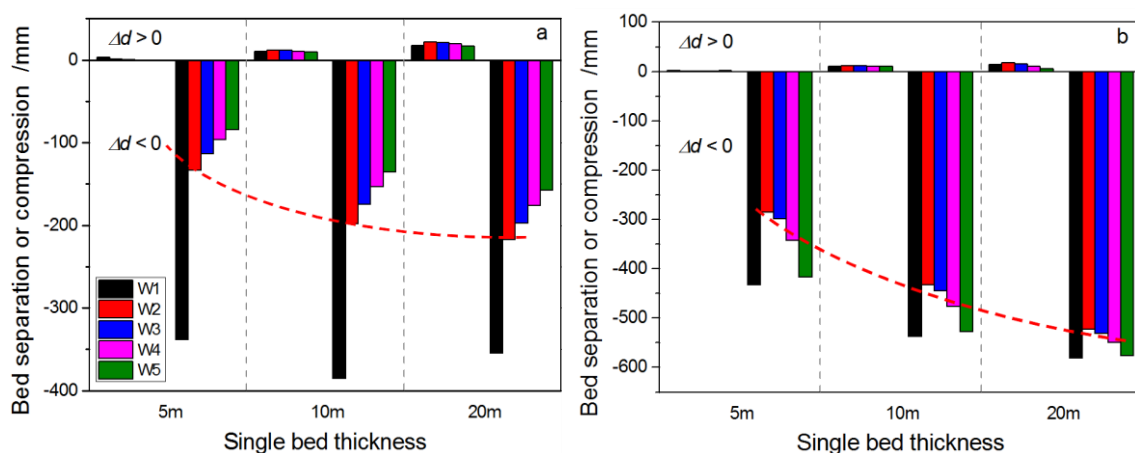


**Figure 4.** Extreme value statistics of bed separation and compression along various well trajectories after the (a) first panel is removed and then (b) twin panels are removed sequentially in cases of various SRLTs.

In these, the left plot (a) and right plot (b) separately represent the deformation magnitudes after the removal first of panel 1 on the left side and then the removal of the second panel on the other side. The peak horizontal shear offset at the weak interface between soft and stiff layers is positively correlated to SRLT (Figure 3a). After the removal of panel 1, the peak horizontal shear offsets (all

single-sensed shear displacements) of various wells grow approximately linearly with increasing SRLT. When SRLT doubles, peak horizontal shear offsets of the various wells less than doubles and grows by only ~40–70%. The closer the candidate well to the first mined panel, the larger the shear offset it undergoes.

After the removal of the second panel (Figure 3b), the cumulative peak horizontal shear offsets of various wells rise approximately logarithmically with increasing SRLT. In other words, the effect of increasing SRLT on the increase in shear offsets at bedding interfaces gradually asymptotes with the peak offsets changing little once SRLT exceeds 10 m. When SRLT increases from 5 m to 10 m, peak horizontal shear offsets of various wells grow by ~20–50%. Extraction of the second panel poses a more severe influence to proximal candidate well trajectories (W5 and W4).

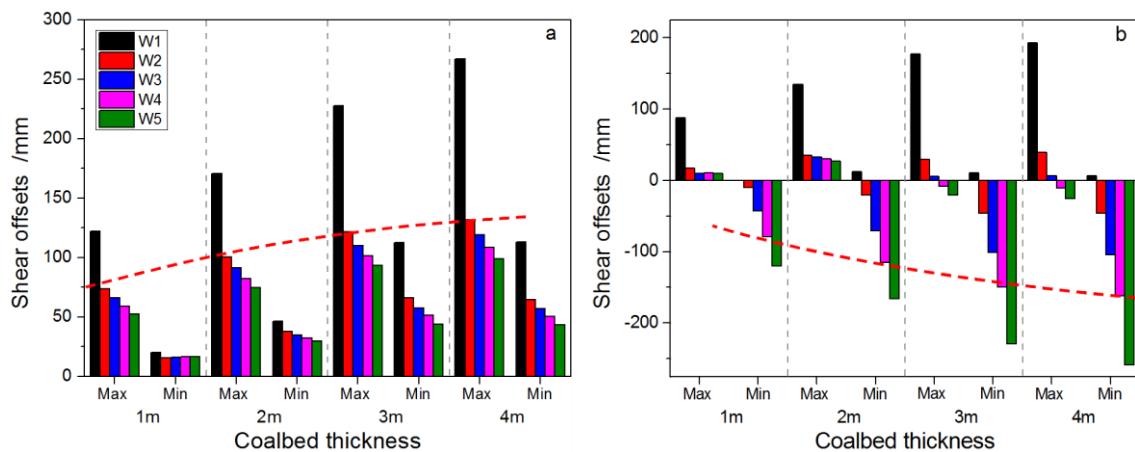
The annular space between the production casing and the coal protection casing in the design used in practice allows for 150 mm [5], for the sake of safety, we limit the threshold of the annular space to 100 mm in the modeling design in this study. This threshold, corresponding to the maximum allowable horizontal shear offset (both the positive and negative ones:  $\pm 100$  mm). A comprehensive consideration of shear offsets of various wells after the sequential extraction of panels flanking the protective pillar indicates that candidate well trajectory W3, deviating from the pillar centerline by 7.5 m is the most viable option as it undergoes the smallest shear offset.

Figure 4 shows that vertical compression dominates over bed separation. Either after the extraction of one panel (Figure 4a) or of both panels (Figure 4b), the vertical delamination and compression of various wells rises approximately logarithmically with increasing SRLT. When SRLT is small (5 m) the flexural stiffness of the rock layer is small. As a result, the adjacent rock layers are more conducive to bending and distortion. Therefore, after the removal of only the first (left) panel, the peak delamination is only 3 mm (scenario I-1, W1). However, when SRLT increases to 10 m and 20 m, the flexural stiffness of the rock layer increases, leading to degraded compatibility between adjacent rock layers. As a result, delamination increases, with the peak delamination reaching 12 mm (scenario I-2, W2) and 21 mm (scenario I-3, W2), respectively (Figure 4a).

With removal of the second panel, vertical delamination remains unchanged or slightly decreases. With regard to vertical compression, well trajectories W1 and W5, which are close to the edges of the pillar and exhibit the largest compression. The closest well trajectory to the coal pillar centerline (W2) has the least vertical compression, being  $-285$ ,  $-432$  and  $-523$  mm for scenarios I-1–I-3, respectively (Figure 4b). Well trajectory W3 shows a slightly larger vertical compression than W2, being  $-299$ ,  $-445$  and  $-531$  mm for scenarios I-1–I-3, respectively (Figure 4b). With an integrated consideration of lateral shear offsets and vertical compression, well trajectory W3 is deemed as the optimal drilling path.

### 3.2. Influence of Seam Mining Height (SMH)

Increasing SMH creates larger mine openings, allowing greater strata movement and inducing greater overburden deformation. Therefore, increasing SMH is more damaging to the stability of small-diameter hydrocarbon wells vertically drilled through longwall mining areas. To examine the effect of SMH on various well deformations, four mining scenarios (scenarios II-1–II-4) are explored. With a fixed burial depth of 300 m, seam thickness in these four scenarios is set as 1, 2, 3 and 4 m, respectively. Figures 5 and 6 separately show the extreme value statistics of lateral shear offsets of the hydrocarbon wells and bed separation or compression along various well trajectories after the twin panels are removed sequentially (for various SMHs).



**Figure 5.** Extreme value statistics of lateral shear offsets of hydrocarbon wells after the (a) first panel is removed and then (b) the second panel is removed for various SMHs.

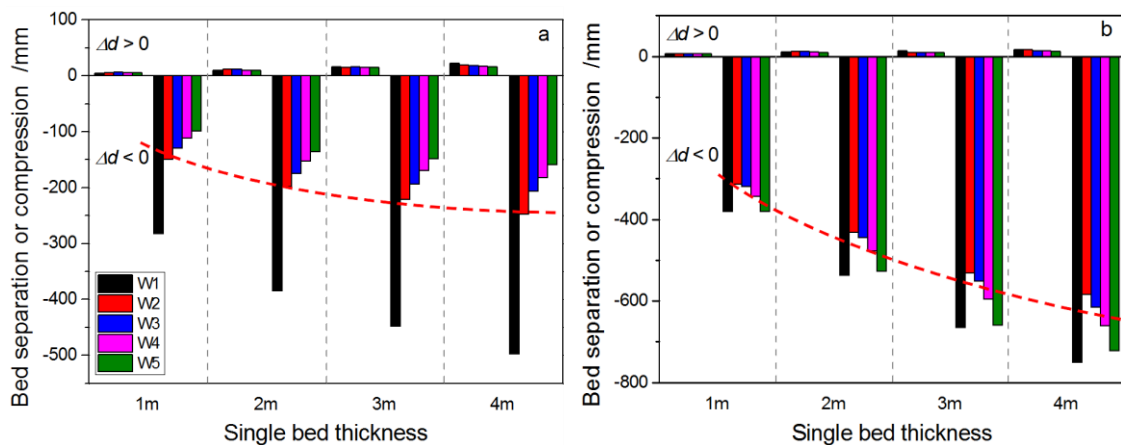


**Figure 6.** Extreme value statistics of bed separation and compression along various well trajectories after the (a) first panel is removed and then (b) the second panel is removed for various SMHs.

The peak horizontal shear offset at the weak interfaces between layers is positively correlated to SMH (Figure 5). As well trajectory W1 is closest to the first mined panel, it suffers the most severe mining-induced influence. The peak horizontal shear offset of W1 grows approximately linearly with increasing SMH after panel one is removed. Horizontal shear offsets of other well trajectories (W2–W5) rise in an approximately logarithmic manner with increasing SMH, either after panel one, or both panels, are extracted. Except for well trajectories W1 and W5, which are closest to the pillar edges, horizontal shear offsets of trajectories W2, W3 and W4 increase by ~30–40% after only the left panel is removed when SMH doubles. However, after the removal of the second panel, horizontal shear offsets of these three trajectories increase by ~41–125% as SMH doubles, indicating that the difference between the effects of increasing SMH on the magnitude of shear offsets of various candidate wells magnifies after the extraction of the second panel. As SMH increases, vertical delamination and compression between beds both grow approximately logarithmically after either one or both panels are removed (Figure 6). Either after one or both panels are removed, the amplifications of vertical compressions on trajectories W1–W5 are of similar magnitude as SMH doubles. The amplification ranges of vertical compressions of the five trajectories are ~32–37% and ~18–29% as SMH increases from 1 m to 2 and 4 m, respectively, after only panel one is removed. The amplification ranges are ~38–41% and ~35–40% as SMH enlarges from 1 m to 2 and 4 m, respectively, after both panels are removed. This demonstrates

that the difference between effects of increasing SMH on the magnitude of vertical compressions of various candidate wells is small.

### 3.3. Influence of Seam Dip Angle (SDA)

When the coal seam is inclined, shear slippage between various rock layers is promoted. Also, both the shear force and frictional force at the interface are correlated to SDA. We explore the influence of SDA on well deformations in a third study group (scenarios III-1–III-4). We define flat coalseams, nearly flat coalseams, gently inclined coalseams and inclined coalseams, as having SDAs of  $0^\circ$ ,  $8^\circ$ ,  $16.7^\circ$ , and  $31^\circ$ , respectively. The non-integer angle is taken for the sake of convenient mesh generation. Considering that most of the peak shear offsets of wells occur within the strata that are dozens of meters above the coalseam [3], we only include interface elements between layers that lie within 200 m above the coalseam. The specific 2D FLAC model is given in Figure 7, with a dip angle of  $31^\circ$  as an example. In each scenario, the vertical distance from the center point of the pillar to the model upper boundary (surface) is 900 m. The panels are set up along dip, advancing along strike (along the axis vertical to the paper view). Extraction occurs of the downdip panel (panel 1) prior to the updip side (panel 2).

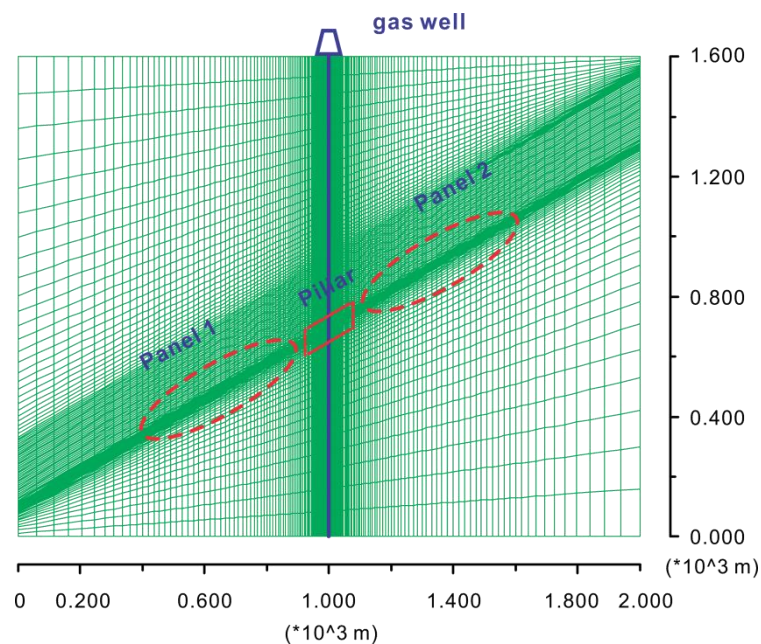


**Figure 7.** A FLAC model to investigate the effect of SDA on well stability (with a dip angle of  $31^\circ$  as an example).

The above analysis shows that well trajectories W1 and W5 suffer more severe mining-induced influence and undergo the largest deformation as they are close to the edges of the pillar. We only perform analysis on the deformation of well trajectories W2, W3 and W4 to make the effect of SDA clearer. Figures 8 and 9 separately show the extreme value statistics of the lateral shear offsets of the wells (relative horizontal displacement), bed separation and compression at the weak interfaces after the two panels are removed sequentially and for various SDAs.

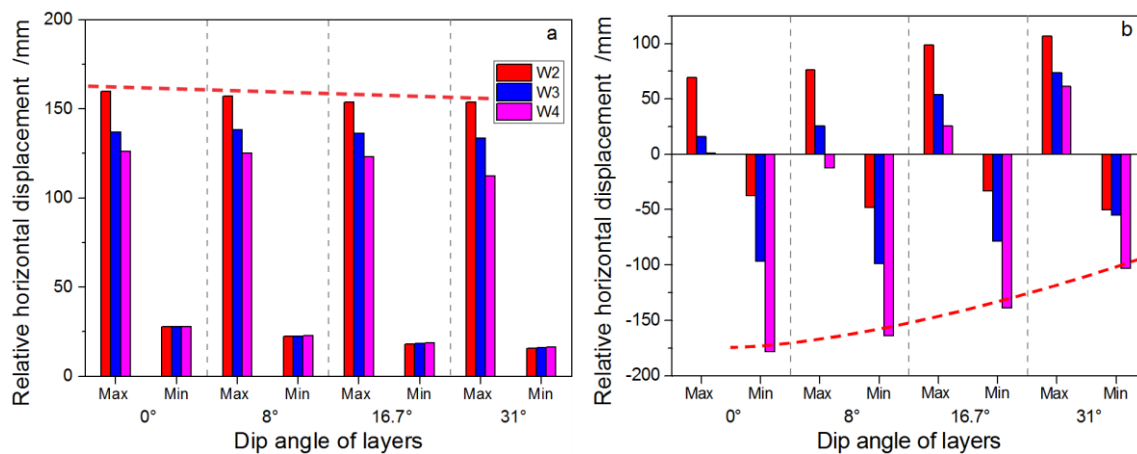


**Figure 8.** Extreme value statistics of relative horizontal displacement of hydrocarbon wells after the (a) first panel is removed and then (b) the second panel is removed for various SDAs.

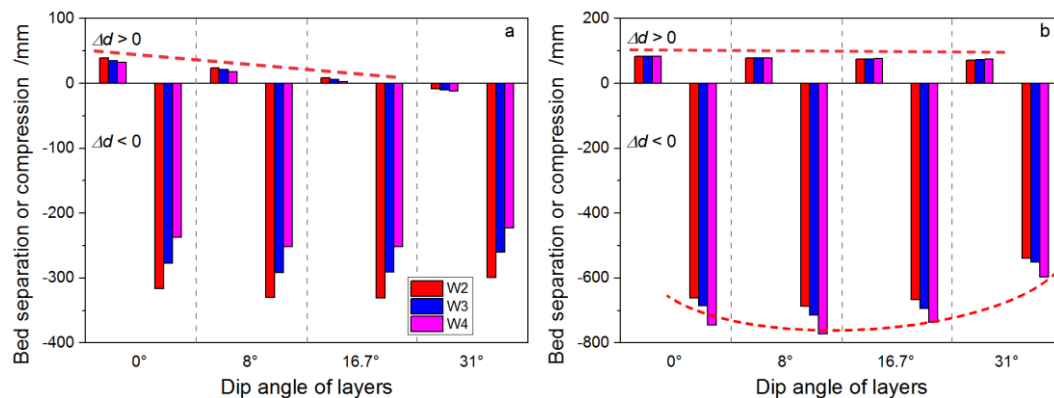


**Figure 9.** Extreme value statistics of bed separation and compression of well trajectories W2–W4 after the (a) first panel is removed and then (b) second panels is removed sequentially in cases of various SDAs.

Shear slippage occurs along the inclined interface between neighboring soft and stiff layers after the removal of the first panel (Figure 8a). The resulting maximum relative horizontal displacements (all single-sensed shear displacements) of well trajectories W2–W4 decrease gently with rising SDA. Therefore, the relative horizontal displacements at interfaces after the extraction of the downdip panel (panel 1) can be considered irrelevant for SDA (0–30°). After the extraction of both panels, the effect of SDA on relative horizontal displacements of various wells varies from the location of the well. More specifically, for well trajectory W2, which is closer to the first mined panel, the peak relative horizontal displacement is still positive; while for well trajectories W3 and W4 that are closer to the later removed panel, the peak relative horizontal displacements reverse to negative. The peak relative horizontal displacement of well trajectory W2 (positive) increases and the peak displacements of well trajectories W3 and W4 (negative) decrease in an approximately logarithmic manner as SDA grows (Figure 8b).

A well would likely not survive an offset greater than its diameter if applied over a short distance—but a relative offset of some fraction of a well diameter could likely be survived—depending on the length over which the distortion is applied. Therefore, given the maximum relative horizontal displacements induced by the slippage of rock layers along the inclined interface, it is considered that increasing SDA is not likely to elevate the risk of shear-induced failure of the well after only the downdip (deep) panel is mined (Figure 8a). In contrast, the final peak relative horizontal displacement of the well resulting from sequential removal of the twin panels decreases with rising SDA (Figure 8b). In other words, risk of shear failure of the well wholly resulting from horizontal shear offset decreases

after the twin panels are removed. However, there is a fixed relation in magnitude between the same horizontal shear offset  $\Delta U$  and its corresponding shear offset along the inclined interfaces (Figure 10a). With a constant  $\Delta U$ , shear offset along the inclined interface increases with rising SDA. As a result, shear-tensile and shear-compression along inclined interfaces between beds (interbedded distortion) elevate, making the well more prone to S-shaped shear failure (or distortion failure, Figure 10b).

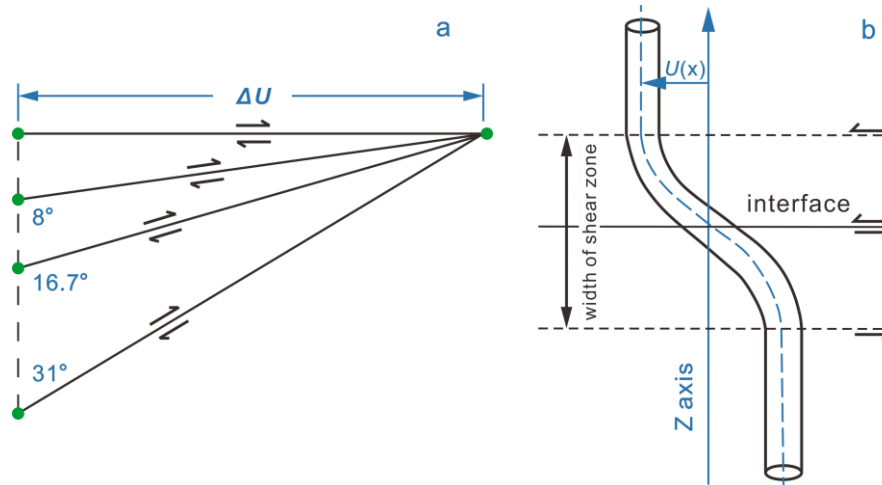


**Figure 10.** Shear offsets along inclined interfaces at different SDA (a) and S-shaped shear failure (b) (modified from [34]) resulting from shear-tensile or shear-compression along inclined interfaces.

Delamination (bed separation) width between soft and stiff layers along the normal direction of the inclined interface narrows with increasing SDA after the removal of only the downdip panel (Figure 10a). When SDA is larger than  $17^\circ$ , delamination at the inclined interface gradually shifts to compression (Figure 10a). After the removal of the twin panels, the peak delaminations between layers in various scenarios all have an apparent rise. Moreover, the delamination width narrows with increasing SDA. However, the difference in magnitude between the wells are insignificant, falling in the range 73 to 83 mm (Figure 10b). Therefore, the delamination between beds is unrelated to SDA after the twin panels are removed. Either after the extraction of the downdip (deep) panel or panels on both sides, all the normal compressions of wells at the inclined interfaces gain an increase prior to a decrease with growing SDA (ranging from  $0$ – $30^\circ$ ). However, the normal compression varies slightly among scenarios III-1–III-3 with the SDA  $< 17^\circ$ , and then decreases by a large percentage as the SDA increases to  $31^\circ$  (Figure 10b). This is mainly due to a larger SDA resulting in a greater gravity force (gravity as a result of strata self-weight) component along the inclined interface and smaller gravity force component in the normal direction. In this circumstance, deformation between inclined beds is mainly manifest in the form of shear.

#### 4. Panel Layout and Mining Optimization for Inclined Coal Seams

The mined space around the vertical hydrocarbon wells, resulting from the removal of panels in an inclined coal seam, are asymmetrical. Mining-induced well deformations can be either ameliorated or aggravated when panels along the strike of the seam are removed in a different sequence (Figure 11a) and panels along the dip of the seam advance in different directions (Figure 11b). Based on the above analysis on the effect of SDA on well deformation at weak interfaces, this section performs an optimization of mining sequence along strike and for panel advance direction along dip.

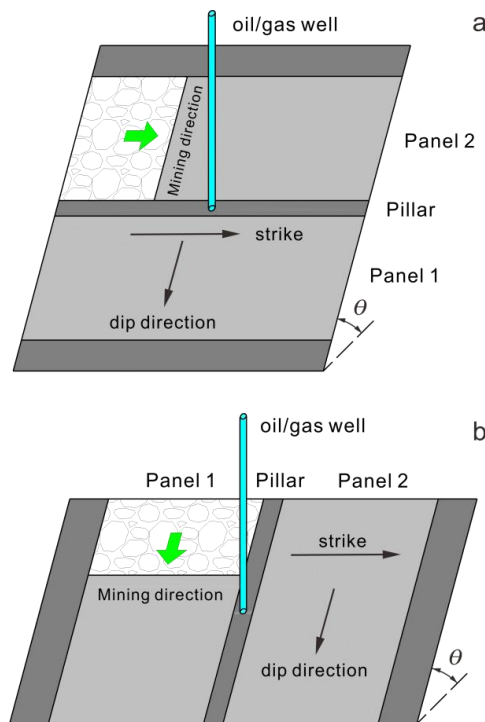


**Figure 11.** Layout of longwall panels along strike (a) and dip direction (b) within an inclined coal seam.

4.1. Optimization on Mining Sequence in Longwall Mining Along Strike

For longwall mining along strike, the extraction sequence in scenarios III-2–III-4 (Table 2) is reversed to examine the effect of mining sequence on well deformations. Thus, removal of the updip panel (shallow, panel 2) now precedes the removal of the downdip panel (deep, panel 1). In the new scenarios, the vertical distance from the pillar center to the model upper boundary (surface) is also 900 m. As indicated in the foregoing, wells at edges of the pillar deform the most. Therefore, we only perform analysis on the deformations of well trajectories W2, W3 and W4. The peak horizontal shear offsets at the weak interfaces between beds in the cases of different extraction sequences are summarized in Figure 12. The peak vertical delaminations occur at the inclined interfaces as summarized in Figure 13.

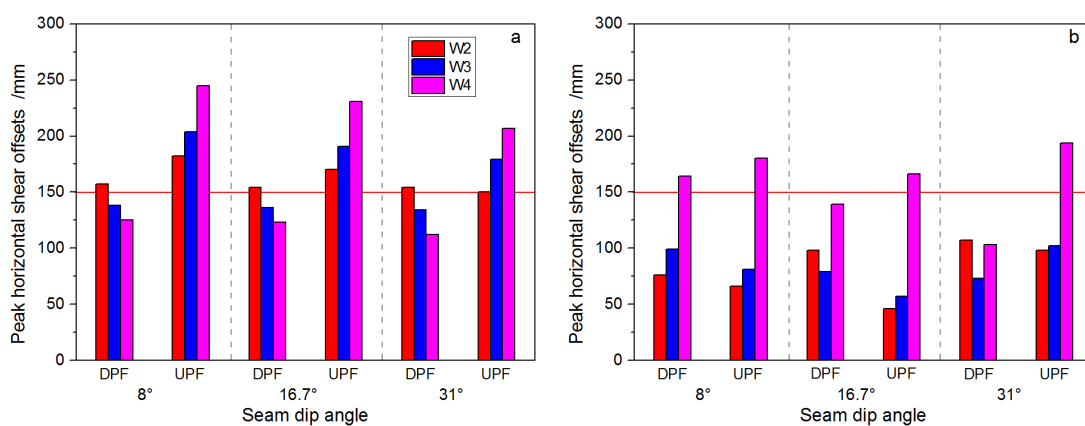


**Figure 12.** Peak horizontal shear offsets of well trajectories W2–W4 for longwall mining along strike after only one panel (a) and then both panels are removed (b) in cases of different extraction sequence. “DPF” represents the downdip panel is removed first and then the updip panel. “UPF” represents the updip panel is removed first and then the downdip panel.

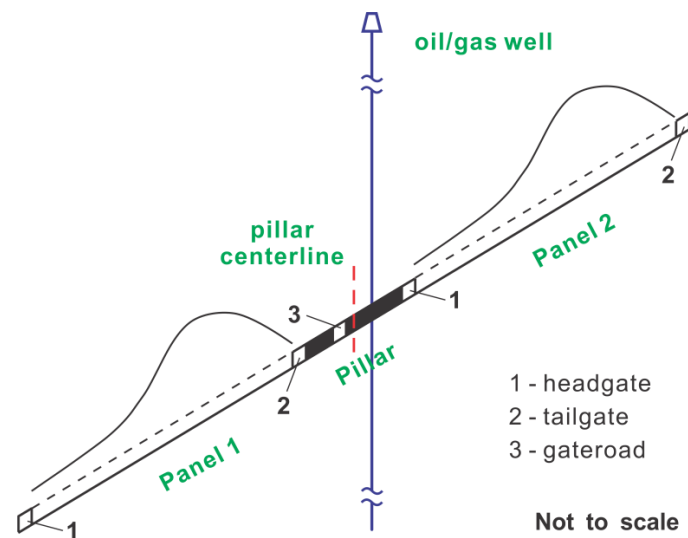


**Figure 13.** Schematic diagram of overburden failure range of longwall panels advance along strike of an inclined coal seam and the optimal location of the oil/gas well.

After only the first panel is removed, peak horizontal shear offsets induced by removing the downdip panel are less than those induced by extracting the updip panel (Figure 12a). However, after the second panel is removed, shear offsets of well trajectories W2–W4 show somewhat complicated characteristics (Figure 12b). (1) For well trajectory W2, extraction of the updip panel prior to the downdip panel results in a smaller residual horizontal shear offset with increasing SDA; (2) Well trajectory W4 shows the opposite results; (3) For well trajectory W3, when SDA is less than  $17^\circ$ , extraction of the updip panel prior to the downdip side results in a smaller residual shear offset; however, when SDA is greater than  $30^\circ$ , the result reverses. A comprehensive analysis of the magnitude of horizontal shear offsets of well trajectories W2–W4 after the sequential extraction of panels flanking the pillar shows that shear deformation of wells induced by the extraction of only one panel dominates in general (horizontal shear offsets resulting from the removal of only one panel are larger than those resulting from the removal of both panels), irrespective of panel extraction sequence. Wells might have already suffered shear failure after the removal of only the first panel, especially when the updip panel is removed first. As a result, from the perspective of effective control of shear offsets of wells, extraction of the downdip panel prior to the updip side favors well integrity; as the resulting shear deformation is the least during the whole mining cycle of the twin panels. In addition, the optimal well trajectory deviates from the centerline of the pillar and is adjacent to the panel that is later removed. The specific deviation distance correlates with SDA. As demonstrated in Figure 12, the optimal well trajectory is W3 when SDA is less than  $17^\circ$ ; when SDA exceeds  $30^\circ$ , the optimal well trajectory is W4, which is closer to the updip panel and is removed later. Actually, this deduction can be indirectly validated by the distribution characteristics of overburden failure of a longwall panel advancing along strike of an inclined seam. That is, fracture development in the overburden above the updip side of the panel is more severe than that in the overburden above the downdip side of the panel (Figure 13). And the heights of the caved zone and fractured zone above the updip side of the panel are larger. So the well deviating from the pillar centerline and close to the updip panel which is later removed is less disturbed by mining of the twin panels.

The peak vertical delaminations that occur at interfaces between neighboring beds are larger as the updip panel is mined first, irrespective of SDA (Figure 14a). After the removal of panels on both sides, however, the difference in vertical delaminations in magnitude between these three wells are minimal regardless of whether the updip or downdip panel is removed first (Figure 14b). It is concluded that the effect of mining sequence on the axial tensile deformation of the well is mainly manifest during extraction of the first panel. Therefore, from the perspective of effective control of

tensile deformation of wells, extraction of the downdip panel prior to the updip side also favors the stability of hydrocarbon wells. In addition, Figures 12 and 14 also demonstrate that, when the downdip panel is mined first, the tensile-induced vertical delamination between layers gradually shifts to compression (Figure 14a) as SDA increases. For example, when SDA is  $31^\circ$ , vertical delamination is not observed within the strata above the pillar after only the downdip panel is removed. Significant vertical delamination at interfaces between beds only occurs after the twin panels are both mined.

In summary, for longwall mining along strike, extraction of the downdip panel prior to the updip side favors the stability of the well, resulting in smaller horizontal shear offset and axial tensile deformation during the sequential removal of the twin panels flanking the central pillar.

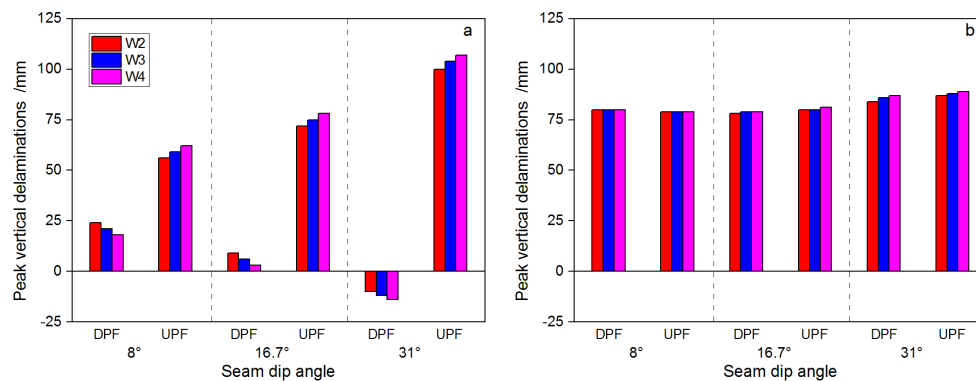


**Figure 14.** Peak vertical delaminations of well trajectories W2–W4 at the inclined interfaces in longwall mining along strike after only one panel (a) and then the second panel is removed (b) in cases of a different extraction sequence. “DPF” represents that the downdip panel is removed first and then the updip panel. “UPF” represents that the updip panel is removed first and then the downdip panel.

#### 4.2. Optimization of Panel Advance Direction in Longwall Mining Along Dip

Different from longwall mining along strike, there are two ways to remove the panel in longwall mining along dip. One is downdip mining (Figure 11b), in which the panel advances along the dip direction of the inclined coal seam. The other is updip mining. Due to a different spatial relation with the hydrocarbon wells drilled through the central pillar, downdip and updip mining may exert different influences on well deformation. In this section, a three dimensional model is employed to investigate the effect of panel advance direction on well stability. Longwall mining along dip is generally applicable for coal seams with a dip angle of  $<12^\circ$ . Otherwise, longwall mining along strike is the preferred option. This is to mitigate such problems as equipment instability, gas accumulation, and drainage inconvenience. Therefore, the SDA is selected as the threshold— $12^\circ$  in the 3D model. Given the symmetry of this geometry we only simulate the extraction of one panel in the 3D model.

The entire 3D model is 450 m wide ( $X$ )  $\times$  400 m long ( $Y$ )  $\times$  317 m high ( $Z$ ) with a flat ground surface (Figure 15). The coal seam is 2 m thick, at a depth of 210–295 m. Overlying 62.5 m thick floor strata, the pillar lies 252.5 m below the model upper boundary (surface) along its vertical centerline. The floor and roof strata are both comprised of alternating soft shale and stiff sandstone. Weak interfaces are set between alternating layers. At the left side of the  $X$  axis, the panel is only 180 m (by half) wide; at the right side, the 270 m wide strata are reserved for the elimination of boundary effect. The panel advances along dip, with the advance length measured by its projection length on the  $Y$  axis. It should be noted that the undermentioned advance lengths all refer to their projection length on the  $Y$  axis. A 50 m wide pillar (three-entry system) is reserved as the protective pillar. Three candidate well trajectories (W2–W4) are also set in the cross-section of the pillar. The cross section is vertical to the  $Y$  axis and intersects the  $Y$  axis at 200 m. Parameters of rock mass and interfaces used in the model are given in Table 2 and the locations of various well trajectories are illustrated in the excerpted frame of Figure 2.

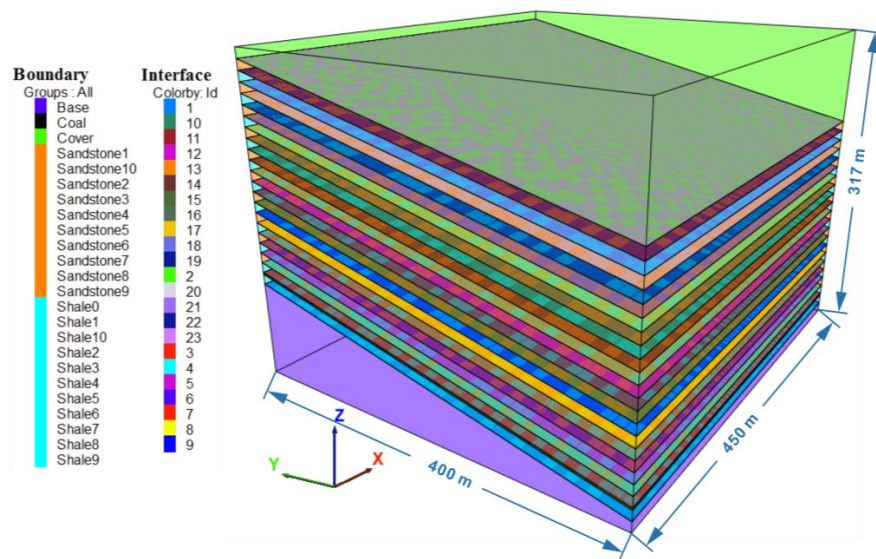


**Figure 15.** A three dimensional model for optimizing the advance direction for longwall mining along dip.

Scenarios IV-1 and IV-2 simulate updip and downdip mining, separately. Analysis is also performed on the deformation of well trajectories W2–W4. As the panel advances along either updip (Figure 16a) or downdip (Figure 16b), the peak horizontal shear offset initially rises rapidly and asymptotes. The peak horizontal shear offsets for well trajectories W2–W4 in the two scenarios show slight differences in magnitude and evolution, indicating that downdip and updip mining have similar effects on shear deformations of the well as the SDA is no greater than  $12^\circ$ . The peak vertical delamination at weak interfaces between beds undergoes a gradual increase prior to a gradual decrease (Figure 17). Similar to the peak horizontal shear offsets, peak vertical delaminations along well trajectories W2–W4, resulting from updip mining (Figure 17a) also resemble those resulting from downdip mining (Figure 17b)—both in magnitude and evolution. These also indicate that updip and downdip mining have similar effects on the axial tensile deformation of wells in longwall mining along dip, with a dip angle of  $<12^\circ$ . Consequently, in such circumstances, either the updip or downdip mining is acceptable.

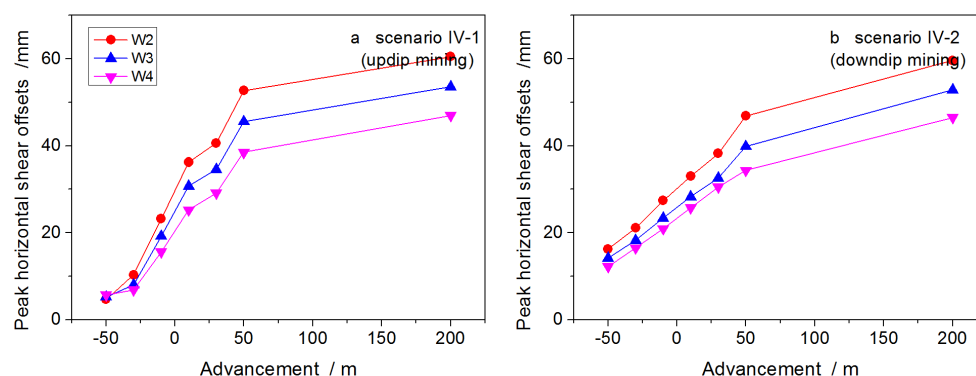


**Figure 16.** Dynamic evolution of peak horizontal shear offsets of well trajectories W2–W4 as the longwall panel advances (a) updip and (b) downdip. The abscissa represents the horizontal distance between the well and the working face after each stage of excavation. Negative magnitudes indicate that the advancing face is ahead of the well and positive magnitudes indicate that the face has passed the well.

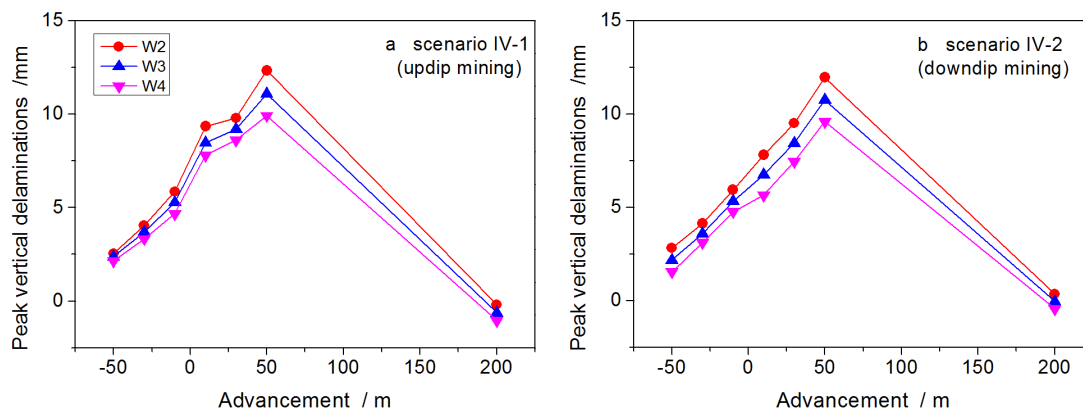


**Figure 17.** Dynamic evolution of peak vertical delaminations along well trajectories W2–W4 as the longwall panel advances (a) updip (b) and downdip. The abscissa represents the horizontal distance between the well and the working face after each stage of excavation. Negative magnitudes indicate that the advancing face is ahead of the well and positive magnitudes indicate that the face has passed the well.

#### 4.3. Recommendations for the Effective Control of Hydrocarbon Well Stability

To protect hydrocarbon wells in longwall mining areas against possible failures, some recommendations regarding coal mining, well construction and peripheral support measures are suggested.

- Spatiotemporal considerations should be given to maintaining well stability. First, mining openings around the wells should be as symmetrical as possible so as to reduce shear and distortion deformation of the wells. Second, if permissible, installation of wells should be delayed. It is better to install wells after mining-induced strata movement stabilizes. For wells installed before mining, coordinated mining of panels surrounding the wells should be performed. A reasonable mining sequence should be designed so as to create symmetrical mining openings. If permissible, simultaneous extraction of the twin panels or synchronous extraction of the twin panels with a small lag distance (Figure 18) is desired to neutralize the deformation induced by the sequential removal of the panels. It should be noted that the twin panels both have a standalone haulage and ventilation system. For inclined coal seams, if longwall mining along strike is employed, the downdip panel should be extracted before the updip panel; if longwall mining along dip is employed (dip angle  $\leq 12^\circ$ ), either updip or downdip mining can be practiced.
- When the panel approaches the well (e.g., within tens of meters), measures such as reducing the mining height and adjusting panel advance rate, will mitigate well deformation. In cases of shallow but thick coal seams, coupled with low strength overlying strata, panels should be advanced slowly so as to mitigate strata movement and stabilize well deformation. For deep coal seams with high strength overlying strata of significant thickness, where strata failure requires more energy and movement or deformation cannot be effectively propagated, panels should be rapidly advanced so as to shorten the duration of roof deformation and shift the disruptive mining-induced influence away from the well.
- Underground longwall mining provides easy access to modify rocks surrounding the hydrocarbon wells and provides the possibility to carry out such measures as wellbore reinforcement and wall rock de-stressing. Prior to panel extraction, grouting reinforcement through the gateroad (entry) can be performed for wall rocks (the pillar that the well penetrates in the six- or nine-pillar configuration, and its roof and floor rocks) around the hydrocarbon wells as wells in these rocks (pillar) are more vulnerable to failure. The reason for employing grouting reinforcement to the pillar is that the plastic zone within the long-weathered pillar (deformation, corrosion and creep) after panel extraction is very likely to expand significantly as the service life of hydrocarbon wells

generally outlives that of the pillar. Grouting can not only plug the fissures within the rock mass, but also strengthen the capacity of the rock to withstand deformation through increasing the cohesion and internal friction angle. Moreover, grouting can improve the mechanical properties of the seam floor and roof interfaces as well as the interfaces between soft and stiff layers, strengthening the cohesive effect at interfaces and restraining shear offsets between beds. In addition, the underlying reason behind the large deformation of the pillar and the adjacent roof and floor rocks is that stresses are highly concentrated when the panel approaches the well. Therefore, borehole pressure relief can be carried out in the stress concentration zones so as to ameliorate the stress condition of the surrounding rocks and reduce deformation of the wells.

- At the base of the main hydrocarbon well, multi-branched horizontal wells are installed, covering an extensive area and serving over a long duration. Therefore, installation of these wells is not only time-consuming, but expensive. For hydrocarbon wells installed in areas where geological conditions are unfavorable and the risk of mining-induced well instability is high, mining methods such as partial extraction, strip extraction, room-and-pillar mining or cut-and-fill mining are recommended.
- For wells to be installed in areas with large existing goafs, exploration wells can be drilled to gain a clear understanding of the condition of the goafs before drilling the hydrocarbon wells. If desired or needed, the goafs may be grouted to improve stability and longevity.

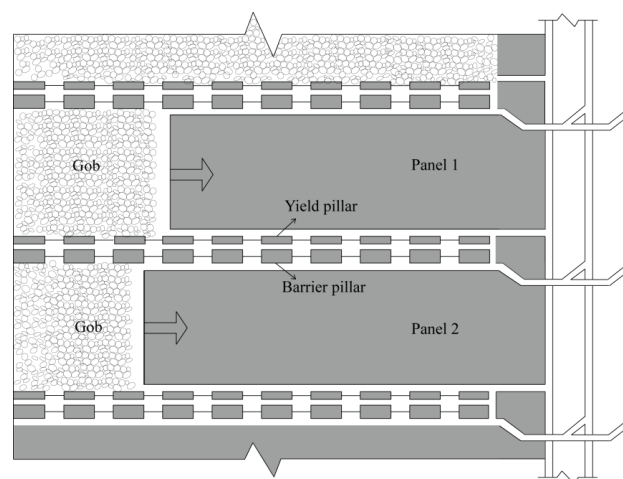


**Figure 18.** Layout of twin longwall panels with standalone haulage and ventilation systems and quasi-synchronous panel advance for the effective control of well stability.

## 5. Conclusions

Due to their small bore diameter (~20–40 cm), as opposed to vertical shafts (~6–10 m), hydrocarbon wells drilled vertically through longwall mining areas are significantly more sensitive to damage by strata movement induced by longwall mining and are vulnerable to severe deformation or potential failure. Stratigraphic conditions are key factors affecting the stability of the hydrocarbon wells. Finite element models investigate the effect of SRLT, SMH and SDA on horizontal shear offset, vertical delamination and compression at the interface between neighboring soft and stiff beds. The influence of sequential extraction of panels flanking the central coal pillar is also investigated. Several recommendations for the effective control of hydrocarbon well stability are proposed. The main conclusions are as follows:

- The peak horizontal shear offset at the weak interface between soft and stiff layers is positively correlated to SRLT. After removal of the first panel, the peak horizontal shear offsets of various wells grow approximately linearly with increasing SRLT; when SRLT doubles, peak horizontal

shear offsets grow only by ~40–70%. After removal of the twin panels, peak horizontal shear offsets of wells rise logarithmically with increasing SRLT. Once the SRLT exceeds 10 m, the effect of SRLT on shear deformation at the bedding interfaces apparently attenuates. When SRLT increases from 5 to 10 m, peak horizontal shear offsets of wells grow by ~20–50%. After either one or both panels are removed, vertical delamination and compression of wells rise approximately logarithmically with increasing SRLT.

- The peak horizontal shear offsets of wells at interfaces are positively correlated to SMH. As well trajectory W1 is closest to the first mined panel, it suffers the most severe mining-induced influence. The peak horizontal shear offset of well trajectory W1 grows linearly with increasing SMH after the first panel is removed. Conversely, peak horizontal shear offsets of the other well trajectories (W2–W5) rise approximately logarithmically with increasing SMH after either one or both panels are removed. The difference between effects of increasing SMH on the magnitude of shear offsets of various wells is magnified after the extraction of the second panel. As SMH increases, vertical delamination and compression between beds both grow approximately logarithmically after either one or both panels are removed. Moreover, the difference between the effects of increasing SMH on the magnitude of vertical compressions of various wells is smaller after both panels are removed.
- SDA exerts an influence on deformation at bedding interfaces. This influence is compounded by the layout of panels inside the inclined coal seam as well as the extraction sequence and the location of the well piercing the pillar. As SDA increases, tensile-induced normal delamination between layers gradually shifts to compression, with shear slip along the inclined interface and compression between beds as the dominant deformation mode. Risk of well shearing due to horizontal shear offset does not increase after either one or both panels are removed. However, shear-tensile/compression at interfaces between beds is elevated, making the well more prone to S-shaped shear failure.
- For longwall panels mined along strike, extraction of the downdip (deep) panel prior to the updip (shallow) side is more favorable for well stability as the horizontal shear offset and vertical delamination between beds are smaller during the whole mining cycle of the twin panels. The offset location of the optimal well trajectory inside the pillar is also correlated to SDA. In general, increasing SDA results in larger deviation of the optimal well trajectory from the pillar centerline, being located closer to the updip panel that is later removed. For longwall mining along dip when SDA is  $<12^\circ$ , both the magnitude and evolution of the peak horizontal shear offset and the peak vertical delamination at weak interfaces resulting from both downdip mining and updip mining are similar as the panel advances, indicating that either method is acceptable.

**Acknowledgments:** Financial support for this work, provided by the Fundamental Research Funds for the Central Universities (2017QNB09), and the Priority Academic Program Development of Jiangsu Higher Education Institutions (PAPD), is gratefully acknowledged.

**Author Contributions:** Xuehai Fu and Xuehua Li conceived and designed the experiments; Shun Liang performed the numerical simulation and analyzed the data; Derek Elsworth helped Shun Liang revise the manuscript; Qiangling Yao helped Shun Liang analyze the data; Shun Liang wrote the paper.

**Conflicts of Interest:** The authors declare no conflict of interest.

## References

1. Feng, X.; Zhang, N.; Chen, X.; Gong, L.; Lv, C.; Guo, Y. Exploitation contradictions concerning multi-energy resources among coal, gas, oil, and uranium: A case study in the Ordos Basin (Western North China Craton and Southern Side of Yinshan Mountains). *Energies* **2016**, *9*, 119. [[CrossRef](#)]
2. Christopher, D.L.; Jaime, K.; David, P.G.; Arnold, G.D.; John, A.H. Trenton and Black River carbonates in the Union Furnace area of Blair and Huntingdon Counties, Pennsylvania: Introduction. In *Field Trip Guidebook for the Eastern Section AAPG Annual Meeting*; John, A.H., Ed.; Pennsylvania Geological Survey: Pittsburgh, PA, USA, 2003.

3. Liang, S.; Elsworth, D.; Li, X.; Yang, D. Topographic influence on stability for gas wells penetrating longwall mining areas. *Int. J. Coal Geol.* **2014**, *132*, 23–36. [[CrossRef](#)]
4. Liang, S.; Elsworth, D.; Li, X.; Fu, X.; Yang, D.; Yao, Q.; Wang, Y. Dynamic impacts on the survivability of shale gas wells piercing longwall panels. *J. Nat. Gas Sci. Eng.* **2015**, *26*, 1130–1147. [[CrossRef](#)]
5. Rostami, J.; Elsworth, D.; Watson, R. *Study of Borehole Stability for Gas Wells in Longwall Mining Areas*; Pennsylvania State University, State College: Hershey, PA, USA, 2012.
6. Scovazzo, V.A.; Russell, P.M. Industry research into gas and oil well protective coal pillar design. In Proceedings of the 32nd International Conference on Ground Control in Mining, Morgantown, WV, USA, 30 July–1 August 2013; pp. 45–52.
7. Su, W.H. Effects of longwall-induced stress and deformation on the stability and mechanical integrity of shale gas wells drilled through a longwall abutment pillar. *Int. J. Min. Sci. Technol.* **2017**, *27*, 115–120. [[CrossRef](#)]
8. Wang, Y.; Watson, R.; Rostami, J.; Wang, J.; Limbruner, M.; He, Z. Study of borehole stability of Marcellus shale wells in longwall mining areas. *J. Petrol. Explor. Prod. Technol.* **2013**, *4*, 1–13. [[CrossRef](#)]
9. Davies, R.J.; Almond, S.; Ward, R.S.; Jackson, R.B.; Adams, C.; Worrall, F.; Herringshaw, L.G.; Gluyas, J.G.; Whitehead, M.A. Oil and gas wells and their integrity: Implications for shale and unconventional resource exploitation. *Mar. Pet. Geol.* **2014**, *56*, 239–254. [[CrossRef](#)]
10. Vidic, R.D.; Brantley, S.L.; Vandenbossche, J.M.; Yoxheimer, D.; Abad, J.D. Impact of shale gas development on regional water quality. *Science* **2013**, *340*, 1235009. [[CrossRef](#)] [[PubMed](#)]
11. Miyazaki, B. Well integrity: An overlooked source of risk and liability for underground natural gas storage. *Geol. Soc.* **2009**, *313*, 163–172. [[CrossRef](#)]
12. Rice, G.S.; Hood, O.P. *Oil and Gas Wells through Workable Coal Beds: Papers and Discussions*; Bureau of Mines: Washington, DC, USA, 1913.
13. Peng, S.; Morsey, K.; Zhang, Y.; Luo, Y.; Heasley, K. Technique for assessing the effects of longwall mining on gas wells—Two case studies. *Trans. Soc. Min. metal. Explor. Inc.* **2003**, *314*, 107–115.
14. Liang, S. Study on the Stability of Vertical Shale Gas Wells Penetrating Longwall Mining Areas. Ph.D. Thesis, China University of Mining and Technology, Xuzhou, China, 2015.
15. Karacan, C.Ö.; Goodman, G. Hydraulic conductivity changes and influencing factors in longwall overburden determined by slug tests in gob gas ventholes. *Int. J. Rock Mech. Min. Sci.* **2009**, *46*, 1162–1174. [[CrossRef](#)]
16. Palchik, V. Localization of mining-induced horizontal fractures along rock layer interfaces in overburden: Field measurements and prediction. *Env. Geol.* **2005**, *48*, 68–80. [[CrossRef](#)]
17. Palchik, V. Experimental investigation of apertures of mining-induced horizontal fractures. *Int. J. Rock Mech. Min. Sci.* **2010**, *47*, 502–508. [[CrossRef](#)]
18. Qian, M. Theoretical study of key stratum in ground control. *J. China Coal Soc.* **1996**, *21*, 225–230.
19. Aadnoy, B.S.; Chenevert, M.E. Stability of highly inclined boreholes. *SPE Drill. Eng.* **1987**, *2*, 364–374. [[CrossRef](#)]
20. Gough, D.I.; Bell, J.S. Stress orientations from oil-well fractures in Alberta and Texas. *Can. J. Earth Sci.* **1981**, *18*, 638–645. [[CrossRef](#)]
21. Haimson, B.C.; Song, I. Laboratory study of borehole breakouts in Cordova Cream: A case of shear failure mechanism. *Int. J. Rock Mech. Min.* **1993**, *30*, 1047–1056. [[CrossRef](#)]
22. Tan, C.P.; Rahman, S.S.; Richards, B.G.; Mody, F.K. Integrated rock mechanics and drilling fluid design approach to manage shale instability. In Proceedings of the SPE/ISRM Rock Mechanics in Petroleum Engineering, Trondheim, Norway, 8–10 July 1998.
23. Tan, C.P.; Willoughby, D.R. Critical mud weight and risk contour plots for designing inclined wells. In Proceedings of the 68th Annual Technical Conference and Exhibition of the Society of Petroleum Engineers, Houston, TX, USA, 3–6 October 1993; pp. 101–115.
24. Zheng, Z.; Kemeny, J.; Cook, N.G.W. Analysis of borehole breakouts. *J. Geophys. Res.* **1989**, *94*, 7171. [[CrossRef](#)]
25. Zoback, M.D.; Moos, D.; Mastin, L.; Anderson, R.N. Well bore breakouts and in situ stress. *J. Geophys. Res. Solid Earth* **1985**, *90*, 5523–5530. [[CrossRef](#)]
26. Bennion, D.B.; Thomas, F.B.; Bietz, R.F. Low permeability gas reservoirs: problems, opportunities and solutions for drilling, completion, stimulation and production. In Proceedings of the SPE Gas Technology Symposium Society of Petroleum Engineers, Calgary, AB, Canada, 28 April–1 May 1996; pp. 117–131.

27. Bjornsson, E.; Hucik, B.; Szutiak, G.; Brown, L.A.; Evans, H.; Curry, D.; Perry, P. Drilling optimization using bit selection expert system and ROP prediction algorithm improves drilling performance and enhances operational decision making by reducing performance uncertainties. In Proceedings of the SPE Annual Technical Conference and Exhibition, Society of Petroleum Engineers, Houston, TX, USA, 26–29 September 2004; pp. 1–6.
28. Clancey, B.; Khemakhem, A.S.; Bene, T.; Schmidt, M. Design, construction and optimization of big-bore gas wells in a giant offshore field. In Proceedings of the SPE/IADC Drilling Conference, Amsterdam, The Netherlands, 20–22 February 2007; pp. 1–9.
29. Supon, S.B.; Adewumi, M.A. Experimental study of the annulus pressure drop in a simulated air-drilling operation. *SPE Drill. Eng.* **1991**, *6*, 74–80. [[CrossRef](#)]
30. Bruno, M.S. Subsidence-induced well failure. *SPE Drill. Eng.* **1992**, *7*, 148–152. [[CrossRef](#)]
31. Chen, J.; Wang, T.; Zhou, Y.; Zhu, Y.; Wang, X. Failure modes of the surface venthole casing during longwall coal extraction: A case study. *Int. J. Coal Geol.* **2012**, *90–91*, 135–148. [[CrossRef](#)]
32. Dusseault, M.B.; Bruno, M.S.; Barrera, J. Casing shear: Causes, cases, cures. *SPE Drill. Complet.* **2001**, *16*, 98–107. [[CrossRef](#)]
33. Liu, C.; Zhou, F.; Yang, K.; Xiao, X.; Liu, Y. Failure analysis of borehole liners in soft coal seam for gas drainage. *Eng. Fail. Anal.* **2014**, *42*, 274–283. [[CrossRef](#)]
34. Whittles, D.N.; Lowndes, I.S.; Kingman, S.W.; Yates, C.; Jobling, S. The stability of methane capture boreholes around a long wall coal panel. *Int. J. Coal Geol.* **2007**, *71*, 313–328. [[CrossRef](#)]
35. Gutierrez, J.J. Estimating Highway Subsidence Due to Longwall Mining. Master’s Thesis, University of Pittsburgh, Pittsburgh, PA, USA, 2008.
36. Jeran, P.; Adamek, V. *Subsidence Due to Undermining of Sloping Terrain: A Case Study*; United States Department of Interior Bureau of Mines: Washington, DC, USA, 1988.



© 2017 by the authors. Licensee MDPI, Basel, Switzerland. This article is an open access article distributed under the terms and conditions of the Creative Commons Attribution (CC BY) license (<http://creativecommons.org/licenses/by/4.0/>).